Tumor suppressor function of Liver kinase B1 (Lkb1) is linked to regulation of epithelial integrity

Johanna I. Partanen[a], Topi A. Tervonen[a,1], Mikko Myllynen[a,1], Essi Lind[a], Misa Imai[a], Pekka Katajisto[b,2], Gerrit J. P. Dijkgraaf[c,3], Panu E. Kovanen[d], Tomi P. Mäkelä[b], Zena Werb[c,4], and Juha Klefström[a,4]

[a]Institute of Biomedicine and Genome-Scale Biology Research Program, Biomedicum Helsinki, University of Helsinki, 00014, Helsinki, Finland; [b]Institute of Biotechnology, University of Helsinki, 00014, Helsinki, Finland; [c]Department of Anatomy, University of California, San Francisco, CA 94143; and [d]Department of Pathology, HUSLAB and Haartman Institute, Helsinki University Central Hospital and University of Helsinki, 00014, Helsinki, Finland

Although loss of epithelial integrity is a hallmark of advanced cancer, it remains poorly understood whether genetic alterations corrupting this integrity causally facilitate tumorigenesis. We show that conditional deletion of tumor suppressor gene Lkb1 (Par-4) in the mammary gland compromises epithelial integrity manifested by mislocalization of cell polarity markers, lateralization of tight junctions, deterioration of desmosomes and basement membrane (BM), and hyperbranching of the mammary ductal tree. We identify the desmosomal BM remodelling serine protease Hepsin as a key factor mediating Lkb1 loss-induced structural alterations in mammary epithelium and BM fragmentation. Although loss of Lkb1 alone does not promote mammary tumorigenesis, combination of Lkb1 deficiency with oncogenic c-Myc leads to dramatic acceleration in tumor formation. The results coupling Lkb1 loss-mediated epithelial integrity defects to mislocalization of serine protease Hepsin and to oncogenic synergy with c-Myc imply that Lkb1 loss facilitates oncogenic proliferation by releasing epithelial cells from structural BM boundaries.

breast cancer | mouse model

Loss of epithelial integrity and tissue organization is a hallmark of all advanced solid cancers (1). However, it is an open question whether the loss of epithelial integrity is causal to tumor progression or is only a tumor phenotype resulting from unrestrained cell proliferation.

Epithelial integrity is maintained by epithelial cell-cell contacts mediated by the apical junctional complex (AJC) composed of tight junctions (TJs) and adherens junctions (AJs) (2, 3). Below the AJC, the basolateral side of epithelial cells harbors desmosomes, which are adhesive intercellular junctions dynamically contributing to epithelial integrity by recruiting intermediate filaments to sites of desmosome assembly (4). The basal side of epithelial cells is bound through integrins to basement membrane (BM), a specialized form of ECM consisting primarily of a laminin and type IV collagen network, nidogen linkers, and proteoglycans (5). The specialized cell junctions and BM enable organized epithelium to sustain apicobasal cell polarity, marked by asymmetrical distribution of macromolecules and intracellular organelles in the cells, which is crucial for normal epithelial functions, such as directional secretion. The interactions of polarized epithelial cells with each other and the microenvironment through the cell junctions and BM not only form the structural basis for epithelial integrity but serve as an epithelial-specific platform for regulation of cell differentiation, signaling, proliferation, cell death, and overall dynamics of epithelial tissue. Therefore, epithelial growth control is tightly linked to the status of epithelial integrity, and it is conceivable that mutations altering epithelial polarity, cell-cell junctions, or BM interactions could act as driver mutations in cancer.

Proteins involved in AJC and BM regulation, such as AJ protein E-cadherin or TJ proteins ZO-1 and Par-3, have been found inactivated or down-regulated in human cancer (6, 7). However, compelling evidence implying a causal role for epithelial integrity genes in tumor progression comes from studies in *Drosophila*. A group of neoplastic tumor suppressor genes is of particular interest, because these genes are important regulators of polarity and, on inactivation, induce ectopic proliferation and tumor formation in *Drosophila* (8). Further studies have revealed tumor suppressor function for a large number of epithelial integrity/polarity regulating genes, such as *bazooka* (Par3) or *cdc42*, in context when these lesions were combined with dominant oncogenes, such as active Ras or Raf (9–11). Early work by Dolberg and Bissell (12) also revealed the importance of epithelial integrity in suppression of v-src–induced transformation in avian embryos. These experiments underline the importance of epithelial integrity as a tumor suppressor mechanism and demonstrate that organized epithelium is capable of restraining the neoplastic activity of activated oncogenes.

Par genes have conserved roles in regulation of cell polarity throughout the metazoa (13). The mammalian homolog of *Drosophila*, Par-4, is a serine-threonine kinase *Lkb1* (liver kinase B1, STK11), which has been implicated in both regulation of epithelial integrity and tumor progression (14). In *Drosophila* oocytes, Lkb1/Par-4 participates in the formation of anterior-posterior axis and apicobasal polarity (15), whereas loss of Lkb1/Par-4 or its downstream target AMPK-α in follicle cells leads to polarity defects and increased proliferation, especially under energetic stress (16). In mammals, forced Lkb1 activity is sufficient to induce polarization of single intestinal epithelial cells (17), and in murine pancreatic acini, loss of *Lkb1* leads to cell polarity defects in conjunction with formation of cystic neoplasms (18). Germline mutations in *Lkb1* gene are causal to hereditary Peutz–Jeghers syndrome, characterized by gastrointestinal polyps and predisposition to several types of cancer, including pancreatic, ovarian, and breast cancer (19). *Lkb1* mutations have also been found in sporadic carcinomas of the lung, pancreas, ovary, and endometrium as well as in cervical cancer (7, 20, 21).

c-Myc is a prototypic oncogene, which enforces cell cycle in cultured cells and induces tumors in mouse models, although often with long latency (22). The cell cycle promoting action of oncogenic c-Myc may be context-dependent. In the mammary epithelial MCF10A cell 3D culture model, structured epithelial organization prevents c-Myc from reinitiating the cell cycle and transforming the acinar structures. This epithelial organization-dependent transformation barrier depends on Lkb1 (7, 23). In the present study, we have analyzed the role of Lkb1 and its interaction with c-Myc in mammary development and tumorigenesis. Our results suggest that Lkb1 has a tumor suppressor function in the mammary gland, which is coupled to the maintenance of epithelial integrity.

Results

Conditional Deletion of *Lkb1* Disrupts Apicobasal Polarity and Epithelial Architecture in Primary Mouse Mammary Epithelial 3D Culture. Primary mouse mammary epithelial cells (MMECs) cultured on reconstituted BM (Matrigel; Becton Dickinson) form apicobasally polarized acinar structures with the AJC and hollow lumens (Fig. S1*A*). To determine whether Lkb1 is necessary for formation of epithelial polarity and glandular organization, we isolated MMECs from *Lkb1^{lox/lox}* mice harboring conditional Lkb1 alleles (24) and infected with adenovirus Cre (AdCre) on low-adhesion plates. The adenoviral infection (Fig. S1*B*) led to loss of Lkb1 protein levels within 72 h after transduction (Fig. 1*A*). We allowed the AdCre-transduced MMECs to form acinar structures in Matrigel and monitored for morphological alterations. After 5 d, the AdCre-transduced *Lkb1^{lox/lox}* 3D acini were abnormally large with irregular morphology (Fig. 1 *B* and *C* and quantification in Fig. S1 *C* and *D*) and were mostly devoid of luminal spaces (Fig. 1*C* and quantification in Tables S1–S3).

We investigated apical polarity in the 3D acini by determining localization of TJ-associated Par-3 and Golgi matrix protein GM130. Par-3 was localized to the apical membrane in the controls but mislocalized to lateral membranes and occasionally to the cytosol in the *Lkb1*-deleted acini (Fig. 1*C*). GM130 stains the Golgi stacks, which reside on the apical side of the nucleus in polarized epithelial cells. However, in *Lkb1*-deficient acini, the stacks were localized to the lateral and even basal sides of the nuclei (Fig. 1*C*, Fig. S1*E*, and quantification in Tables S1–S3). Higher magnification images also revealed abnormal laterally extended expression of the TJ marker ZO-1 (Fig. 1*D* and quantification in Tables S1–S3). Transmission electron microscopy (TEM) analyses confirmed the absence of lumens in acini lacking Lkb1 and revealed small luminal spaces, or microlumens, in the structures (Fig. S1*F*). Although the cells facing the microlumens still had some apical identity, as indicated by apical brush border and AJC structures (Fig. 1*E*), we observed laterally extended TJ domains (Fig. 1 *E* and *F*) consistent with the laterally expressed TJ marker ZO-1 (Fig. 1*D*). Other derangements of cell junctions, such as multiple desmosomes, were evident in central parts of the *Lkb1*-deficient acini (Fig. S1*F*). In summary, *Lkb1* is necessary for formation of normal epithelial polarity and glandular architecture.

Fig. 1. Lkb1 is required for mammary epithelial integrity. (*A*) Western blot showing loss of Lkb1 protein in isolated *Lkb1^{lox/lox}* MMECs 72 h after AdCre recombinase infection. (*B*) Morphology of the AdCre-infected *Lkb1^{lox/lox}* MMECs grown in 3D culture for 5 d. (Scale bar: 100 μm.) (*C*) Day 10 *Lkb1^{lox/lox}* 3D acini immunostained for Par-3 and GM-130. (Scale bar: 20 μm.) (*D*) Day 10 *Lkb1^{lox/lox}* 3D acini immunostained for E-cadherin and ZO-1. Asterisks denote the luminal side in close-up images. (Scale bar: 20 μm.) (*E*) TEM images of control and AdCre-infected *Lkb1^{lox/lox}* 3D acini. The red arrowheads mark the ends of TJs, and the black arrowhead denotes a desmosome. (Scale bar: 0.5 μm.) (*F*) Quantification of TJ length. Mean and SD values were calculated from at least three independent experiments.

Partanen et al.

Spontaneous Branching and Abnormal BM in the Lkb1-Deficient 3D Acini. We observed that about 40% of the AdCre-infected *Lkb1^lox/lox* 3D acini but none of the controls spontaneously developed protruding hollow branches (Fig. 2 *A* and *B*). These structures were similar to structures developed in 3D MMECs stimulated to undergo branching morphogenesis by exogenous FGF-2 (25) (Fig. S2*A*). Because increased branching of mammary epithelium is associated with deregulation of BM remodeling enzymes (26), we next investigated the BM structure in the *Lkb1*-deficient 3D acini by scanning electron microscopy (SEM). The SEM images of control MMEC 3D acini grown "on top" of the Matrigel showed a smooth and even BM layer surrounding the control acini, whereas the AdCre-infected *Lkb1^lox/lox* acini had rough and irregular BM (Fig. 2*C*). By immunostaining, the control acini were surrounded by a continuous layer of the BM proteins Laminin-332, Collagen IV, and nidogen, whereas the *Lkb1*-deficient acini had reduced or uneven, gapped distribution of BM markers (Fig. 2*D* and Fig. S2 *B* (quantification) and *C*). The data suggest that *Lkb1* is required for formation of proper BM structure.

Conditional Deletion of *Lkb1* Leads to Hyperbranching and Deterioration of BM in the Mouse Mammary Gland. To determine whether loss of *Lkb1* perturbs epithelial integrity in vivo, we used a conditional gene KO strategy to inactivate *Lkb1* alleles in the adult mouse mammary gland. We crossed the *Lkb1^lox/lox* mice with mice transgenic for whey acidic protein promoter (W)-controlled Cre recombinase (27). The W-Cre transgene is expressed in alveolar cells of the mammary epithelium with modest activity in mid-pregnancy and high activity during lactation (27). We confirmed the allelic deletion of *Lkb1* by genomic PCR and quantitative PCR (qPCR) analysis of mRNA expression (Fig. S3 *A* and *B*). The conditional *Lkb1* alleles were recombined into null alleles in the mammary glands of parous W-Cre;*Lkb1^lox/+* and W-Cre;*Lkb1^lox/lox* mice as well as in the virgin W-Cre;*Lkb1^lox/lox* mice (Fig. S3*A*) as a result of minor W-Cre activation during the estrous cycle (28). Concurrently, the *Lkb1* mRNA levels were reduced in the mammary epithelial cells of both virgin and parous W-Cre;*Lkb1^lox/lox* mice (Fig. S3*B*).
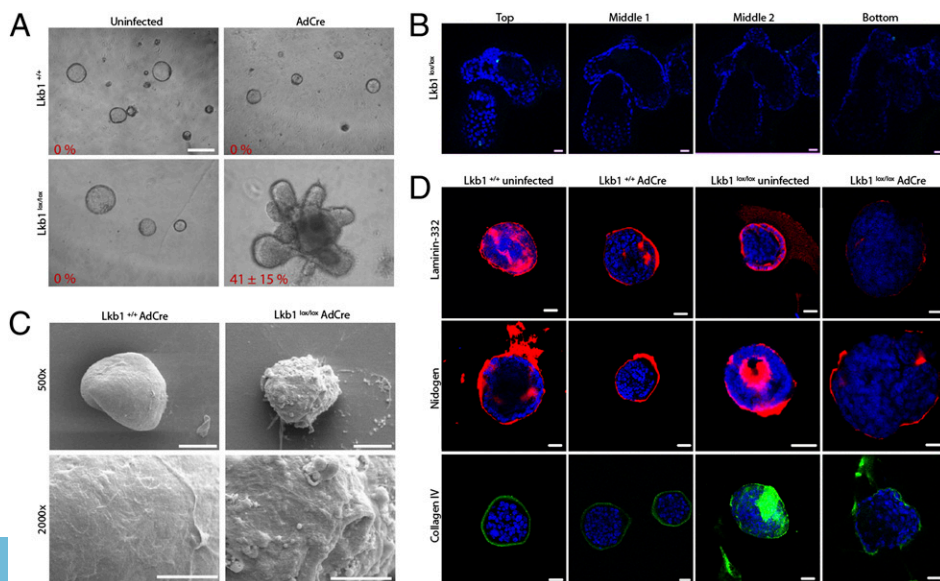
The ultrastructure of the mammary epithelium of multiparous W-Cre;*Lkb1^lox/lox* mice was relatively normal (Fig. S3*D*); however, notably, the mammary glands of virgin W-Cre;*Lkb1^lox/lox* mice showed a marked increase in lateral side branches (Fig. 3*A* and quantification in Fig. S3*C*). In both parous and virgin *Lkb1*-deficient glands, the stroma was altered, as indicated by thick eosinophilic regions (Fig. 3*B* and quantification in Tables S4 and S5) enriched in Collagen I and III surrounding the mammary epi-

thelium (Fig. 3*C* and Fig. S3*E*). Furthermore, similar to the Lkb1-deficient 3D acini, the pattern of BM Collagen IV staining was discontinuous around the *Lkb1*-deficient mammary epithelial ducts (Fig. 3*C* and quantification in Tables S4 and S5). In summary, deletion of *Lkb1* leads to increased ductal side-branching, overproduction of interstitial collagens, and defective BM in the mouse mammary gland.
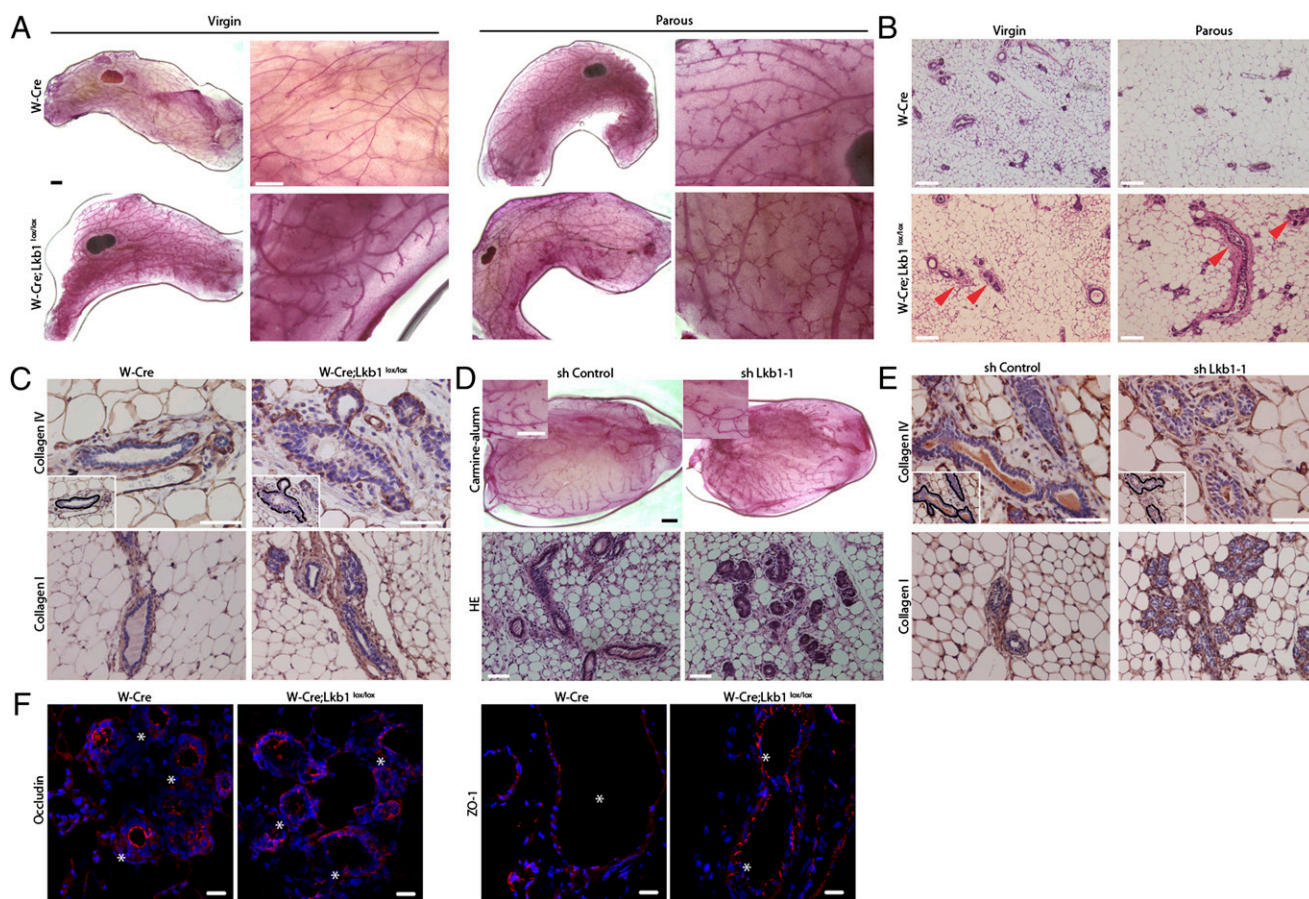
Reconstitution of Mammary Ductal Tree from Lkb1-Deficient Progenitor Cells Results in Hyperbranching and BM Deterioration Defects. To validate the link between Lkb1, hyperbranching, and BM deterioration, we isolated MMECs harboring mammary progenitor cells and transduced the cells with high-concentration lentivirus expressing one of two different validated Lkb1 silencing shRNAs or nontargeting control shRNA. The transduced MMECs were transplanted to cleared mammary fat pads of 3-wk-old recipient FVB inbred mice to reconstitute mammary gland (29). At 15 wk after the transplantations, about 70% of the transplanted glands had prominent ductal outgrowths spanning the whole fat pad. In agreement with our findings in the W-Cre;*Lkb1^lox/lox* glands, silencing of Lkb1 (Fig. S3*F*) induced hyperbranching in the ductal tree (Fig. 3*D*). The ducts exhibited discontinuous Collagen IV staining (Fig. 3*E*) and were encircled by eosinophilic thickenings (Fig. 3*D*) enriched in Collagens I and III (Fig. 3*E*). Thus, both shRNA-mediated silencing and allelic KO of *Lkb1* results in hyperbranching and deterioration of BM in the virgin mouse mammary gland.

We also explored the apical cell polarity in vivo by immunostaining frozen sections from control and W-Cre;*Lkb1^lox/lox* glands for the TJ markers occludin and ZO-1 (Fig. 3*F* and quantification in Fig. S3*G*). The occludin staining was apical, and ZO-1 staining was apical and occasionally diffuse in the control glands. In contrast, both occludin and ZO-1 localized in the apical and lateral sides of the cells in the W-Cre;*Lkb1^lox/lox* samples. These results imply that loss of *Lkb1* leads to lateral orientation of TJs in the epithelium of the mammary gland and that *Lkb1* is required for normal epithelial cell polarity.

Loss of Lkb1 Cooperates with c-Myc in Mammary Tumorigenesis. We did not observe tumors in the Lkb1-deficient parous mice during 1 y of follow-up, in keeping with previous studies demonstrating that loss of Lkb1 may promote mammary tumorigenesis only weakly (30). Because Lkb1-dependent perturbation of mammary epithelial integrity may not induce tumorigenesis directly, we explored whether the compromised integrity could enhance the competence of oncogenic c-Myc to drive unscheduled proliferation (7, 23). We

Fig. 2. Loss of Lkb1 results in spontaneous branching and disruption of BM. (*A*) Phase-contrast images of day 10 control and *Lkb1^lox/lox* 3D acini showing branching. Percentages indicate the number of acini with branching structures. (Scale bar: 100 μm.) (*B*) Z-stack of confocal images to visualize hollow cavities in branching *Lkb1^lox/lox* 3D acini. The mitotic activity is visualized with phospho-Histone H3 antibodies. (Scale bar: 20 μm.) (*C*) SEM images of AdCre-infected control and *Lkb1^lox/lox* acini grown on top of Matrigel. (Scale bars: 50 μm in images with a magnification of 500×, 20 μm in images with a magnification of 2,000×.) (*D*) Day 10 control and AdCre-infected *Lkb1^lox/lox* 3D acini immunostained for Laminin-332, nidogen, or Collagen IV show a discontinuous staining pattern surrounding LKB1-lacking acini. (Scale bar: 20 μm.)

Fig. 3. Loss of Lkb1 in the mouse mammary gland results in hyperbranching, deterioration of BM, and disruption of apical polarity. (*A*) Carmine-alum staining of mammary gland whole mounts from virgin and parous control and W-Cre;*Lkb1*$^{lox/lox}$ mice shows ductal hyperbranching. (Scale bars: 1 mm; close-up images, 500 μm.) (*B*) H&E-stained paraffin sections of virgin and parous W-Cre;*Lkb1*$^{lox/lox}$ glands show eosinophilic thickenings (arrowheads). (Scale bar: 100 μm.) (*C*) Collagen IV and I immunostaining of paraffin sections of parous W-Cre;*Lkb1*$^{lox/lox}$ glands. (Scale bar: 50 μm.) (*Insets*) Black line delineates pattern of Collagen IV staining. (*D*) Carmine-alum–stained mammary gland whole mounts and H&E-stained paraffin sections of genetically engineered ductal trees expressing either shControl or shLkb1-1 construct. (Scale bar: 1 mm.) Close-up images (cropped from the original image) show ductal side branching (59.6 branch points in the shControl and 71.3 branch points in shLkb1 counted as in Fig. S3C from 4 animals per group, 3–4 image fields per sample with a magnification of 40×). (Scale bar: 200 μm.) (*E*) Collagen IV and I immunostaining of paraffin sections of shControl and shLkb1-1–expressing glands. (Scale bar: 50 μm.) (*Inset*) Black line delineates pattern of Collagen IV staining. (*F*) Parous control and W-Cre;*Lkb1*$^{lox/lox}$ glands immunostained for Occludin and ZO-1. Asterisks mark the lumens. (Scale bar: 20 μm.)

crossed mice expressing transgenic c-Myc under control of whey acidic protein (WAP) promoter (31) with the W-Cre;*Lkb1* $^{lox/lox}$ mice. The intercrossing of F1 hybrids resulted in tritransgenic mice carrying W-Myc and W-Cre alleles as well as one or two conditional *Lkb1* alleles (W-Myc;W-Cre;*Lkb1*$^{lox/+}$ or W-Myc;W-Cre;*Lkb1*$^{lox/lox}$; hereafter, Myc/Lkb1-). To induce the WAP promoter, we allowed the mice to undergo two sequential pregnancies. We observed that c-Myc expression was elevated in the parous W-Myc mammary glands and remained elevated in the tumors after pregnancy (Fig. S4A), as reported earlier (32). The tumors from Myc/Lkb1- mice exhibited reduced levels of Lkb1 mRNA and protein (Fig. S4B).

Although control mice (W-Myc;W-Cre) developed palpable mammary tumors at 6 mo of age (Fig. 4A), the combined Myc overexpression and Lkb1 loss dramatically accelerated mammary tumorigenesis, shortening the mean latency of tumor formation to 2.5 mo. The Myc/Lkb1- mice typically developed tumors during the first pregnancy and often in the nulliparous state. Loss of one *Lkb1* allele also potentiated c-Myc–dependent tumorigenesis, albeit less efficiently than homozygous loss of *Lkb1* (Fig. 4A).
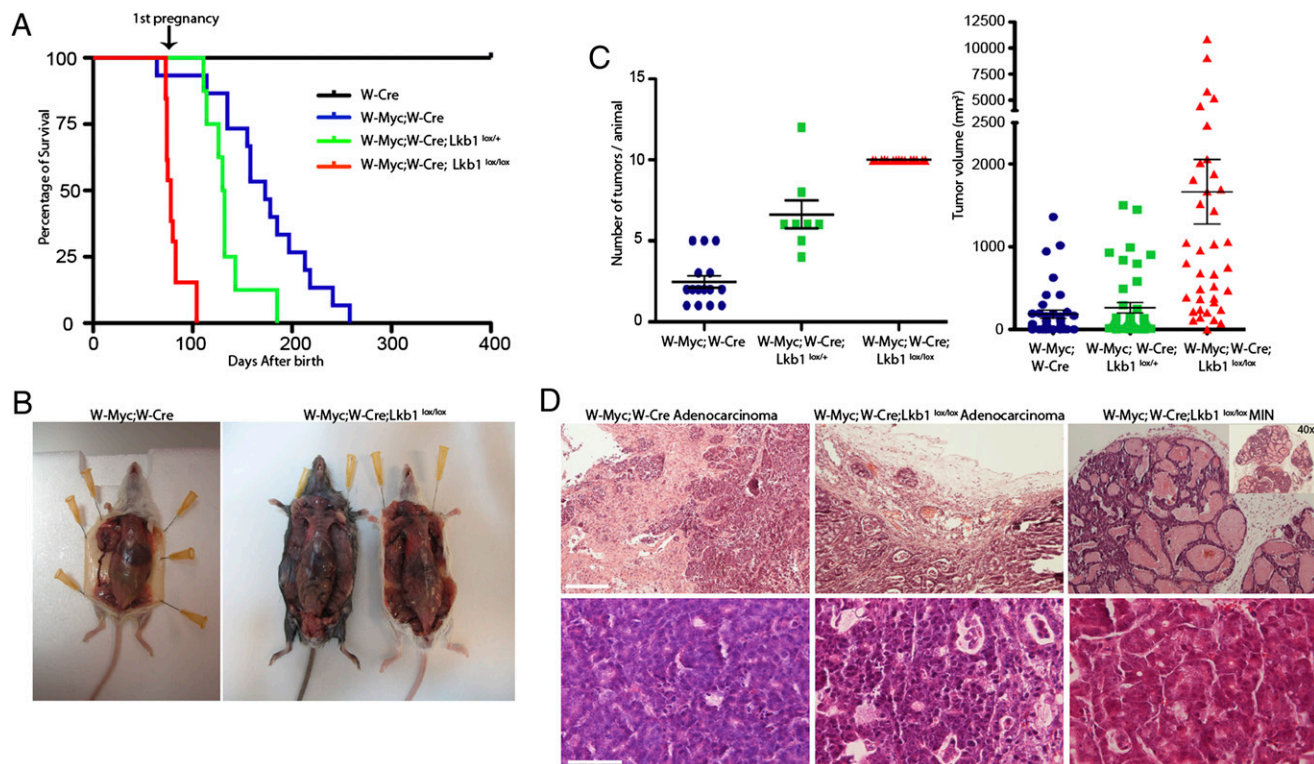
The allelic loss of *Lkb1* also altered the multiplicity, morphology, and histopathology of tumors developing in the W-Myc mice. In contrast to the Myc-induced solitary tumors typically affecting one

or two glands, the Myc/Lkb1- mice developed tumors in all 10 mammary glands (Fig. 4B) and the tumor volume was over sixfold larger (Fig. 4C). Also, a hemizygous loss of *Lkb1* increased tumor multiplicity. The W-Myc–induced tumors were focal or multifocal adenocarcinomas demonstrating invasive behavior and pulmonary metastases in 10% of mice, as reported previously (31, 33). The tumors arising in the Myc/Lkb1- glands were not focal but were instead diffuse, affecting the whole gland (Table S6). Moreover, the Myc/Lkb1- males were predisposed to mammary tumor formation, although with lower penetrance (65%) and multiplicity (mean of 3.6), possibly attributable to low activity of WAP promoter in males and/or lack of tight regulation of the heterologous WAP system (32). Taken together, the data underscore striking cooperation between c-Myc activation and *Lkb1* loss in mammary tumorigenesis.

Loss of Lkb1 Induces Coalescence of Ducts and Alveolar Units, Creating Tumors with Unique Features. In contrast to Myc-induced focal adenocarcinomas, which appeared with long latency, only half of the rapidly forming Myc/Lkb1- tumors were adenocarcinomas and half were classified as mammary intraepithelial neoplasia (MIN) (Fig. 4D and Table S6). The MIN lesions were cytologically high grade and indistinguishable from adenocarcinomas (34) (Fig. 4D and Table S6). The outer tumor mass facing the stroma still had

Fig. 4. c-Myc and loss of Lkb1 cooperate in mammary tumorigenesis. (*A*) Kaplan–Meier survival analysis of Myc and Myc/Lkb1- mice. The arrow approximates the first pregnancy. (*B*) Photographs of mammary tumors in W-Myc;W-Cre and Myc/Lkb1- mice. Note a solitary single tumor in the W-Myc;W-Cre mouse and the multiplicity of tumors in the two Myc/Lkb1- mice. (*C*) Tumor multiplicity (*Left*) and volume (*Right*) in the mice. (*D*) Tumor histopathological findings. Shown is an H&E-stained adenocarcinoma from a Myc mouse as well as adenocarcinoma and MIN from Myc/Lkb1- mice. The large magnification shows nuclear pleomorphism and cellular atypia identical in all tumors. However, the adenocarcinoma-defining invasive front was absent in MIN (images with magnifications of 100× and 40×). (Scale bars: 200 μm in images with a magnification of 100×, 50 μm in images with a magnification of 400×.)

intact BM; however, within the tumors, the epithelial structures coalesced, forming large sacs that gave a distinct morphology to these tumors (Fig. 4*D* and Fig. S4*C*).

The rapid tumorigenesis accompanied by coalescing epithelial structures and irregularities in BM suggested involvement of Lkb1-dependent epithelial integrity aberrations in mammary tumor progression. Furthermore, loss of Lkb1 did not inhibit Myc-induced apoptosis, indicating no major role for apoptosis in tumor progression (Fig. S4 *D* and *E*). Enhanced alveolar development is commonly observed in the mouse mammary glands exposed to Myc activity either in conjunction with or independent of pregnancy (33, 35). Indeed, the nontumorous glands from W-Myc mice typically showed hyperplastic alveolar units, clearly separated from each other by BM, as indicated by a layer of Collagen IV (Fig. 5*A*). The glands from Myc/Lkb1- mice had rare areas where glandular epithelial structures were present. These structures were large, dilated, and filled with luminal secretions. Notably, no clear borders could be observed between the structures because the epithelium was negative for Collagen IV (Fig. 5*A*). The coalescing phenotype did not depend on pregnancy because the phenotype was also observed in tumors from virgin mice. The nontumorous glands from W-Myc;W-Cre;*Lkb1*^lox/+^ mice contained supernumerary alveolar units, which mostly had intact BM, as indicated by a Collagen IV layer (Fig. 5*A*).
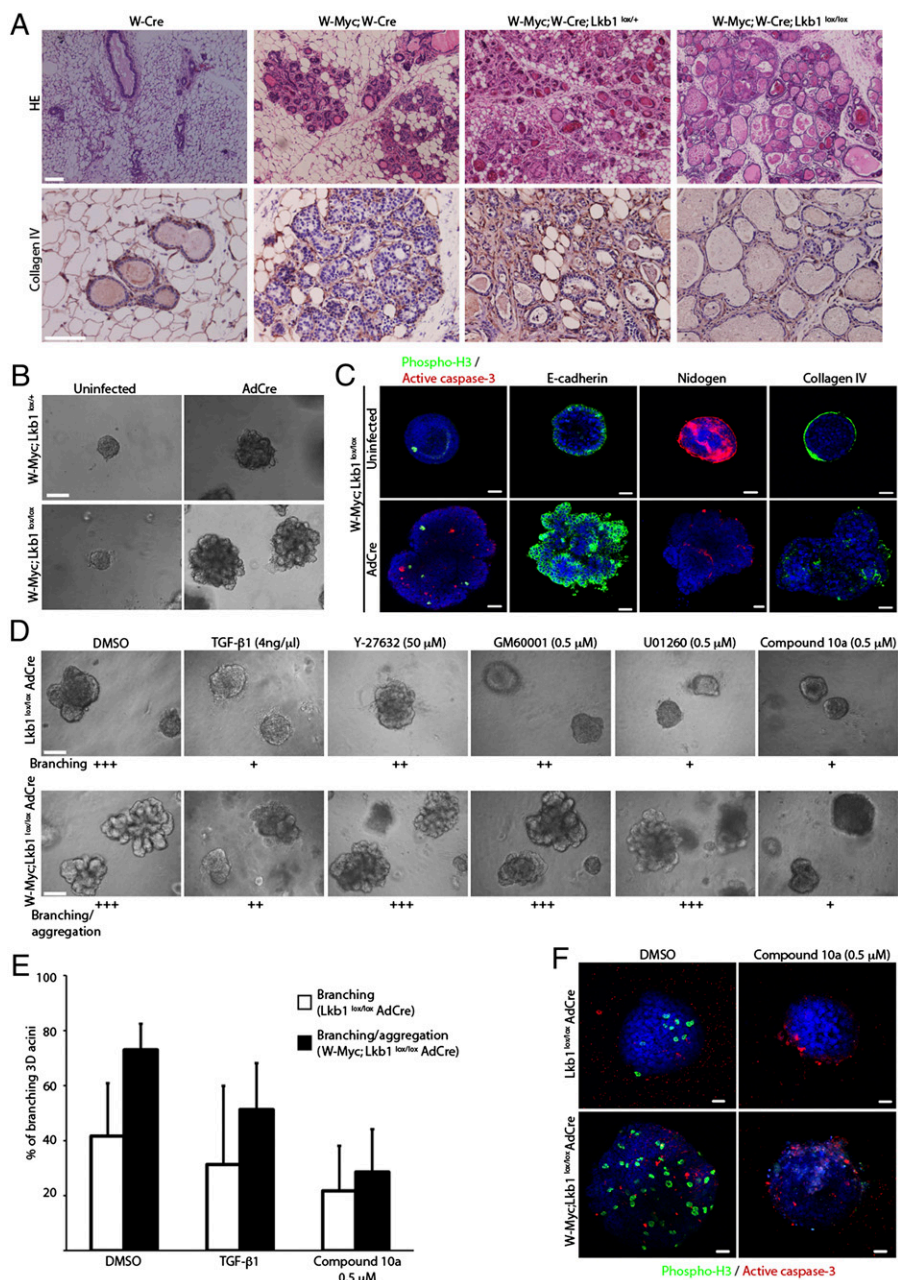
To determine the Myc/Lkb1- phenotype in 3D acini, we isolated MMECs from W-Myc;*Lkb1*^lox/lox^ mice, deleted *Lkb1* alleles in vitro by AdCre, and subsequently allowed 3D structures to form for 5 d. W-Myc was expressed in vitro at levels high enough to induce a transformed phenotype (Fig. S5 *A* and *B*). The acinar structures with c-Myc and deletion of both *Lkb1* alleles were larger than controls and showed a complex, transformed phenotype with a multiacinar appearance and numerous branch-like protrusions

(Fig. 5*B*). These structures had high proliferative and apoptotic activity as well as unevenly distributed and diminished BM proteins nidogen and Collagen IV, indicating deterioration of BM (Fig. 5*C*).

In summary, our data suggest that Myc overexpression in the short term induces alveolar proliferation and apoptosis in the mammary gland without compromising the epithelial structure. We postulate that the accelerated tumorigenesis in Myc/Lkb1-mammary glands is attributable to a convergence of Lkb1-dependent disintegration of epithelial architecture and BM with the Myc-dependent enforced alveolar proliferation phenotype (see Fig. 7*F*).

Lkb1-Dependent Loss of Epithelial Integrity Involves Trypsin-Like Serine Protease Activity. The in vitro phenotypes recapitulated epithelial integrity alterations observed in the Lkb-deficient and Myc/Lkb1- mammary glands, which prompted us to use rescue of 3D structure integrity as a robust approach to identify molecular pathways involved in the disintegration of epithelial structures and promotion of tumorigenesis. We targeted pathways implicated in regulation of branching morphogenesis and ECM/epithelial integrity (36–38). We isolated MMECs from *Lkb1*^lox/lox^ and W-Myc;*Lkb1*^lox/lox^ mice and transduced the cells with AdCre. Thereafter, the 3D structures were grown for 3 d and treated with inhibitors of matrix metalloproteinases (MMPs), MAPK, and RhoA/Rho-associated protein kinase (ROCK) pathways, trypsin-like serine proteases, and TGF-β1. All these additions inhibited the spontaneous branching induced by loss of *Lkb1* (Fig. 5*D*). The most potent suppression of branching was obtained with TGF-β1 and with the inhibitors of MAP/ERK kinase (MEK) and trypsin-like serine proteases. By contrast, the branching/aggregation phenotype of Myc/Lkb1-deficient 3D acini was only inhibited by TGF-β1 and inhibition of trypsin-like serine proteases (Fig. 5 *D* and *E*). Fur-

www.manaraa.com

Fig. 5. Loss of Lkb1 leads to coalescence of BM-defective alveoli in vivo and trypsin-like serine protease-dependent spontaneous branching and aggregation of 3D acini. (*A*) H&E-stained nontumorous glandular tissue sections from W-Myc;W-Cre, W-Myc;W-Cre;*Lkb1*$^{lox/+}$, and Myc/Lkb1- mice illustrate the tissue ultrastructure and presence or absence of BM by Collagen IV staining. (Scale bar: 50 μm.) Note the alveolar multiplication typical for Myc-overexpressing glands (W-Myc;W-Cre) and intact BM surrounding the alveoli. The images of Myc/Lkb1- glands show merged epithelial structures and absence of BM. (Scale bar: 100 μm.) (*B*) Phase-contrast images of AdCre-treated W-Myc;*Lkb1*$^{lox/+}$ and W-Myc;*Lkb1*$^{lox/lox}$ MMECs grown in 3D culture for 5 d show extensive aggregation and branching of acinar structures. (Scale bar: 100 μm.) (*C*) Immunostaining of W-Myc;*Lkb1*$^{lox/lox}$ 3D acini shows increased apoptosis (active Caspase-3) and mitotic activity (phospho-Histone-H3) and reduced levels of BM components nidogen and Collagen IV in the aggregated Myc/Lkb1-deficient acini. Ultrastructure of acini is revealed by E-cadherin staining. (Scale bar: 20 μm.) (*D*) Trypsin-like serine protease activity mediates Lkb1-dependent spontaneous branching and aggregation of 3D acini. AdCre-treated *Lkb1*$^{lox/lox}$ and W-Myc;*Lkb1*$^{lox/lox}$ 3D acini were allowed to form for 3 d and subsequently treated for 48 h with the following effectors/inhibitors: TGF-β1, ROCK inhibitor Y-27632, MMP inhibitor GM6001, MEK inhibitor UO126, and trypsin-like serine protease inhibitor Compound 10a. (Scale bar: 100 μm.) The level of spontaneous branching (*Lkb1*$^{lox/lox}$) or branching/aggregation (W-Myc;*Lkb1*$^{lox/lox}$) of 3D acini in each treatment was evaluated on day 5 by visually comparing treated 3D acini with DMSO control (+++, extensive branching; ++, moderate branching; +, slight or no branching). (*E*) Quantification of TGF-β1 and Compound 10a-mediated inhibition of spontaneous branching and branching/aggregation. The 3D acini were treated as in *A*, and the mean and SD values were calculated from three independent experiments. (*F*) Compound 10a treatment inhibits mitotic activity without significant effect on apoptosis in the *Lkb1*$^{lox/lox}$ and W-Myc;*Lkb1*$^{lox/lox}$ 3D acini. (Scale bar: 20 μm.)
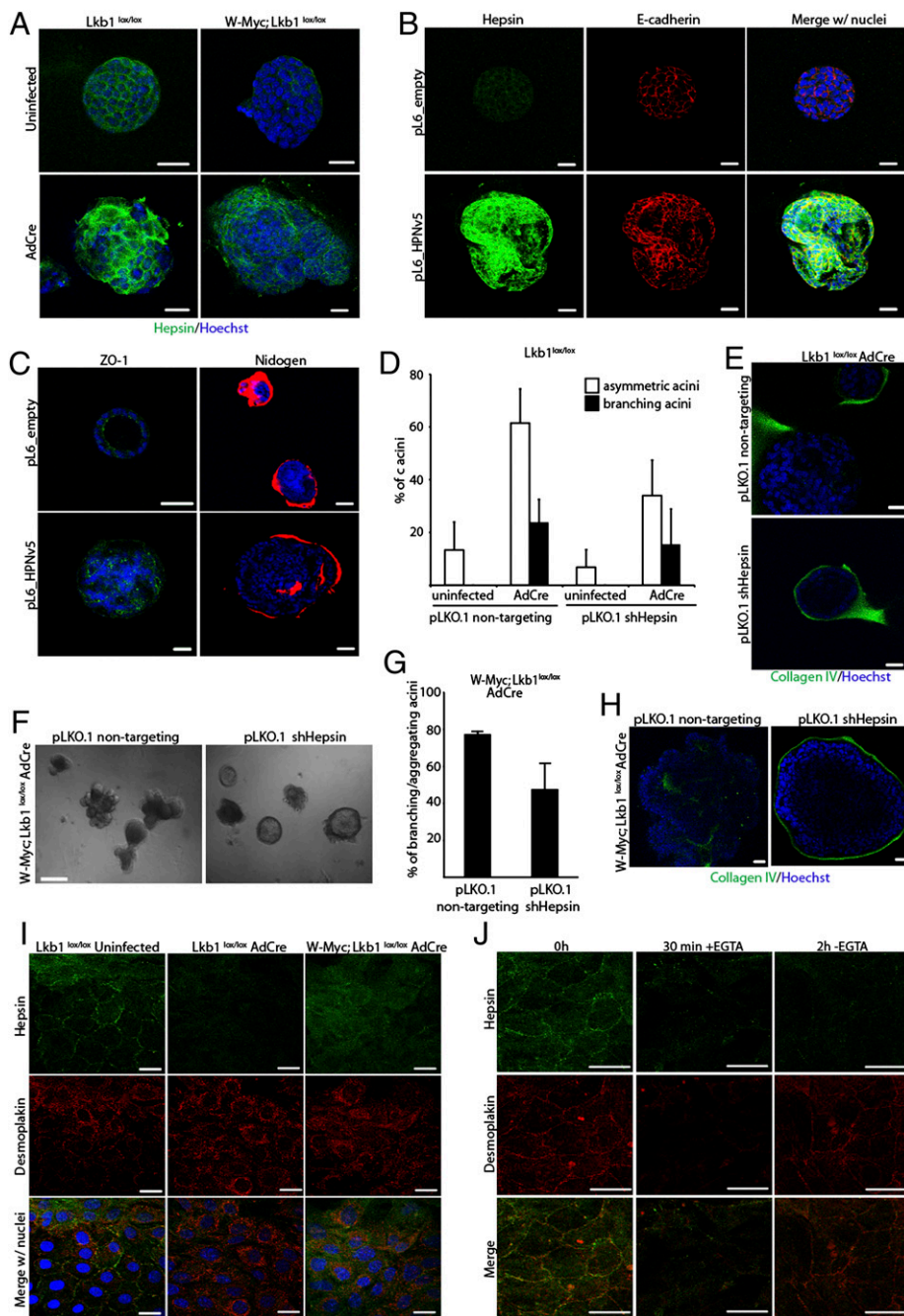
thermore, the trypsin-like serine protease inhibitor Compound 10a (39) inhibited the cell cycle without promoting apoptosis in 3D acini, confirming that the inhibition targeted cell proliferation (Fig. 5*F*). We focused on trypsin-like serine proteases because little is known about the interactions between these proteases and epithelial integrity regulation/tumor progression.

Loss of Lkb1 Induces Redistribution of the Type II Transmembrane Serine Protease Hepsin, Which Mediates BM Degradation and Oncogenic Transformation. Hepsin, a type II transmembrane trypsin-like serine protease, is normally expressed at the cell surface, whereas it is overexpressed in certain tumors, especially prostate and ovarian tumors, where Hepsin often exhibits strong cytosolic staining (40, 41). We observed that the immunostaining of Hepsin was enhanced and redistributed from cell-cell borders toward diffuse cytosolic expression on loss of Lkb1 in the 3D acini (Fig. 6*A*). Similar changes were observed in the transformed 3D acini with oncogenic Myc and loss of Lkb1.

To test whether Hepsin could perturb epithelial integrity functionally, we overexpressed V5-tagged Hepsin in MMECs. The overexpressed Hepsin localized to both membranes and cytosol (Fig. 6*B* and Fig. S6*A*). The 3D MMEC acini overexpressing Hepsin exhibited a disorganized ultrastructure (Fig. 6 *B* and *C*). The acini had asymmetrical morphology with filled lumens and occasional microlumens as well as perturbed cell polarity, as indicated by loss of apical ZO-1 staining. The discontinuous pattern of nidogen staining indicated deterioration of BM (Fig. 6*C*). Thus, deregulated expression of Hepsin is sufficient to disrupt epithelial integrity.

We then asked whether Hepsin is required for epithelial phenotypes induced by loss of Lkb1 alone or in combination with Myc. We identified a lentiviral shRNA construct, which silenced Hepsin in the normal murine mammary gland MMEC line and in 3D MMECs (Fig. S6 *B* and *C*). Silencing of Hepsin partially rescued the epithelial phenotypes induced by Lkb1 deficiency, as indicated by improved acinar symmetry and reduced branching
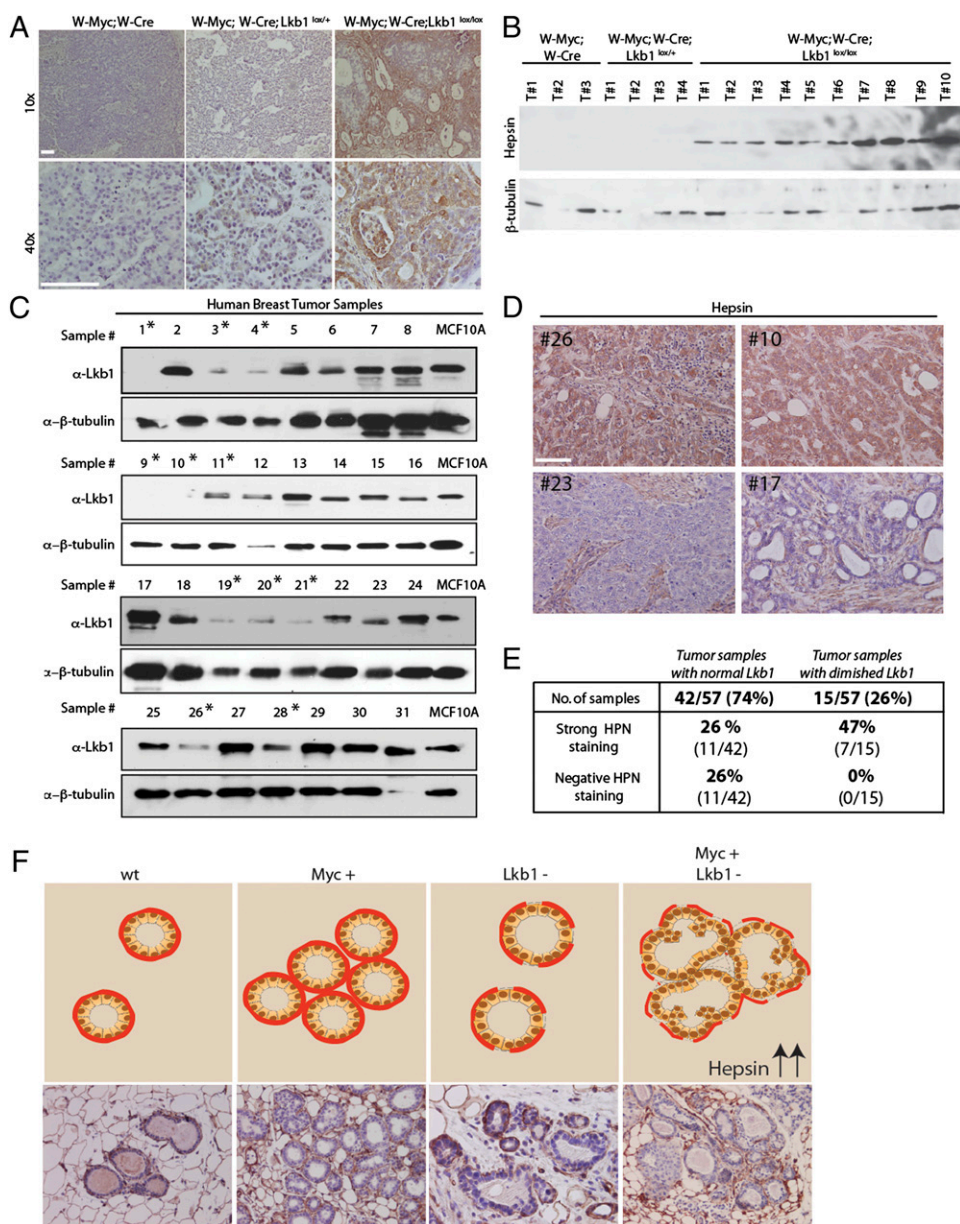
Partanen et al.

Fig. 6. Type II transmembrane serine protease Hepsin mediates epithelial integrity and BM defects as well as transformation in Lkb1-deficient 3D acini. (*A*) Loss of Lkb1 (*Lkb1$^{lox/lox}$* and W-Myc;*Lkb1$^{lox/lox}$*) in the 3D acini enhances immunostaining of Hepsin and leads to its redistribution from cell borders to cytosol. (Scale bar: 20 μm.) (*B*) Overexpression of Hepsin in 3D MMEC acini (3-d culture) results in Hepsin redistribution and asymmetrical, distorted acinar morphology as well as filling of the luminal space. E-cadherin visualizes the cell borders in figures. (Scale bar: 20 μm.) (*C*) Overexpression of Hepsin in 3D MMEC acini induces disruption of apico-basal polarity and deterioration of BM as indicated by mislocalization of ZO-1 and uneven staining of nidogen. (Scale bar: 20 μm.) (*D*) shRNA silencing of Hepsin rescues loss of Lkb1-induced epithelial phenotypes. The graph shows mean and SD values from three independent experiments. (*E*) shRNA silencing of Hepsin rescues loss of Lkb1-induced BM defect. (Scale bar: 20 μm.) (*F*) Phase-contrast images of day 10 W-Myc;*Lkb1$^{lox/lox}$* MMEC acini transduced with pLKO.1 shHepsin demonstrate partial reversion of the branching/aggregation (transformation) phenotype. (Scale bar: 100 μm.) (*G*) Mean and SD of branching/aggregating acini quantitated from three independent experiments. (*H*) shRNA silencing of Hepsin rescues BM defect in acini with Myc and Lkb1 loss double lesion. (Scale bar: 20 μm.) (*I*) Loss of Lkb1 induces concomitant loss of desmoplakin and Hepsin from desmosomal junctions. (*Left*) Colocalization of desmoplakin and Hepsin in cell-cell borders. (*Center* and *Right*) Ablation of desmoplakin and Hepsin form cell-cell borders in AdCre-infected *Lkb1$^{lox/lox}$* and W-Myc;*Lkb1$^{lox/lox}$* MMECs grown in 2D cell culture. (Scale bar: 20 μm.) (*J*) Dissociation of Hepsin and desmoplakin from cell-cell junctions on calcium depletion. For the calcium switch assay, MMECs were treated with EGTA for 30 min, after which EGTA was removed and the cells were incubated for an additional 2 h. (Scale bar: 20 μm.)

(Fig. 6*D* and Fig. S6*D*) as well as reestablishment of BM structure (Fig. 6*E* and quantification in Fig. S6*E*). Moreover, silencing of Hepsin rescued the branching/aggregation phenotype of Myc/Lkb1-deficient 3D acini; both the morphology (Fig. 6 *F* and *G*) and BM defect (Fig. 6*H* and quantification in Fig. S6*E*) were partially reverted by Hepsin ablation. Together, these data indicate a role for Hepsin in mediating the BM defects and epithelial disorganization caused by Lkb1 deficiency. Moreover, the "transformed" branching/aggregation phenotype of Myc/Lkb1-deficient 3D acini is attributable to deregulated Hepsin.

Desmoplakin anchors intermediate filaments to desmosomal plaques and is an obligate component of functional desmosomes (Fig. 6*I* and Fig. S6*F*). In keeping with earlier observations of desmosomal localization of Hepsin (40), we found that Hepsin partially colocalizes with desmoplakin. Although desmoplakin and Hepsin resided in cell junctions of normal 3D MMECs, loss of Lkb1 led to disappearance of these proteins from cell-cell borders (Fig. 6*I*, *Center* and Fig. S6*G*). Also, overexpression of Myc coupled with Lkb1 loss led to disappearance of junctional desmoplakin and redistribution of Hepsin from cell-cell junctions to the cytosol (Fig. 6*I*). When we perturbed cell-cell junctions of WT MMECs by calcium depletion, we observed that deterioration of cell junctions led to disappearance of Hepsin from cell borders (Fig. 6*J* and Fig. S6*H*). Intriguingly, subsequent restoration of cell-cell junctions (Fig. S6*H*) under normal calcium conditions reversed junctional localization of desmoplakin, whereas Hepsin remained mislocalized (Fig. 6*J*). These data show that loss of Lkb1 induces desmosomal defects and that such junctional defects associate with mislocalization of Hepsin.

We then analyzed tumor samples from W-Myc;W-Cre, W-Myc;W-Cre;*Lkb1$^{lox/+}$*, and Myc/Lkb1- mice (*n* = 11 tumors from each

Fig. 7. Hepsin is deregulated in Lkb1-deficient mouse mammary tumors and human breast cancer. (*A*) Loss of Lkb1 in tumor-prone mammary glands (Myc/Lkb-) leads to overexpression of Hepsin. (Scale bar: 50 μm.) (*B*) Western blot analysis of Hepsin expression in W-Myc;W-Cre, W-Myc;W-Cre;*Lkb1*$^{lox/+}$, and W-Myc;W-Cre;*Lkb1*$^{lox/lox}$ tumors. (*C*) Western blot analysis of LKB1 protein levels in 31 unselected human breast cancer samples obtained as frozen samples during diagnosis. Human mammary epithelial MCF10A cell line is used as a reference, and β-tubulin is used as a loading control. Tumors with reduced or nondetectable LKB1 levels are marked with an asterisk. (*D*) Hepsin expression in representative human breast cancer samples. Hepsin staining was scored in the carcinoma cells as strong (>40% of the cells positive, nos. 26 and 10), moderate (15–40% of the cells positive, no. 17) or negative (<15% of the cells positive, no. 23) (note that the stromal cells but not the carcinoma cells are positive). (Scale bar: 100 μm.) (*E*) Scoring table consolidating *C* and *D* (*P* = 0.026, Fisher's exact test). (*F*) Model explains how Lkb1-dependent loss of epithelial integrity contributes to mammary tumorigenesis. Activation of oncogenic c-Myc in mammary epithelial cells induces hyperproliferation, which leads to development of surplus alveolar units. However, these early-stage malignancies remain contained within the hyperplastic layers of epithelial cells by BM. Although loss of Lkb1 leads to degradation of BM, it does not endow cells with full competence for unscheduled proliferation; therefore, Lkb1 loss alone is only weakly or not tumorigenic in the mammary gland. Combined action of c-Myc and loss of Lkb1 unleash rapid mammary tumor formation by c-Myc driving unscheduled cell cycle and loss of Lkb1 releasing these cells from structural boundaries established by BM. BM is marked in the schematic figure with a red line and in the photomicrographs (20×) by brown immunostaining for Collagen IV.

group) for Hepsin expression (Fig. 7*A*). The majority (75%) of tumor samples from W-Myc;W-Cre mice were negative for Hepsin. In contrast, 64% of the tumors from Myc/Lkb1- mice manifested strong widespread immunostaining of Hepsin (Fig. 7*A*). Tumor samples from Myc/Lkb1 hemizygous mice were also Hepsin-positive, but staining was less intense (70% moderate positive). Hepsin protein expression was also consistently elevated in the Myc/Lkb1-tumors, as measured by Western blot analysis (Fig. 7*B*). The relatively mild lysis conditions used in these experiments revealed only the 31-kDa active form of Hepsin, thus not distinguishing whether Myc/Lkb1- lesions enhance proteolytic processing of Hepsin or up-regulate Hepsin expression. Therefore, we analyzed subcellular fractions of MMECs and found increased levels of both full-length and processed Hepsin in membrane fractions from the Myc/Lkb1-MMECs (Fig. S6*I*). These data indicate that Myc/Lkb1- lesions promote strong deregulation, involving both mislocalization and overexpression of Hepsin in primary epithelial cells and mouse mammary tumors.

Reduced LKB1 Expression Is Associated with Hepsin Deregulation in Human Breast Cancer. *LKB1* mutations are rare in sporadic breast cancers; however, diminished LKB1 protein expression has been reported in advanced breast tumors and papillary mammary carcinomas (42–44). Therefore, we determined the LKB1 protein expression by Western blot analysis in 57 unselected clinical breast cancer samples (Fig. 7 *C–E* and Table S7). LKB1 was expressed in 74% of the tumor samples at levels comparable to nontransformed MCF10A mammary epithelial cells (Fig. 7*E*). However, 26% (15 of 57) of the tumor samples expressed low or undetectable LKB1 levels (Fig. 7*E*). We determined the level of Hepsin expression by immunostaining sections from the same samples. Strong Hepsin expression was observed in 18 (32%) of 57 samples (Fig. 7 *D* and *E*), and rest of the samples showed moderate or negative Hepsin expression (Table S7). Interestingly, in the group of tumors expressing low/undetectable LKB1 levels (*n* = 15), 47% were strongly Hepsin-positive and none were Hepsin-negative (Fig. 7*E*). By comparison, in the group of tumors expressing LKB1 (*n* = 11), 26% of the samples were strongly Hepsin-positive and 26% were Hepsin-negative. Thus, reduced LKB1 protein levels are associated with deregulation of Hepsin in human breast cancer.

Partanen et al.

Discussion

Par-4/Lkb1, like other Par proteins, centrally controls establishment of the apicobasal polarity and epithelial integrity in invertebrates. In mammals, Lkb1 is necessary for formation of proper epithelial architecture and cell orientation (18, 23), and it is sufficient to program apical identity in cultured cells (17). Nonetheless, it has remained unclear how loss of the Lkb1 polarity function, which affects individual cells, translates into defects in epithelial tissue integrity and how these defects might be linked to tumor progression. We find that loss of Lkb1 in the mouse mammary gland leads to defects in cell polarity, TJ positioning, and desmosomal integrity and that it leads to deterioration of BM. The culprit for BM deterioration is a serine protease, Hepsin, which becomes liberated from junctional complexes by loss of Lkb1. In a mammary tumorigenesis model driven by strongly cooperating Lkb1 loss and Myc overexpression, we find that mislocalized, overexpressed Hepsin is present in a majority of tumors and that such deregulated Hepsin is critical for development of tumor phenotype in organoids, arguing that the tumor suppressor function of Lkb1 is coupled to maintenance of epithelial integrity.

Loss of Lkb1 Damages Junctional Complexes, Which Liberates Hepsin to Induce Deterioration of BM. Loss of Par-4 induces lateralization and multiplication of AJs in *Drosophila* photoreceptor cells, which lack TJs (45), providing an interesting parallel to our findings of TJ lateralization in mammary epithelial cells, and this suggests that genetic interaction between Lkb1 and AJC positioning is an evolutionary conserved feature. However, spatial mispositioning of TJs as such does not explain how Lkb1 deficiency leads to multiple epithelial integrity defects. In agreement with Miao et al. (40), we find that spatial localization of Hepsin partially overlaps with the desmosomal junction protein desmoplakin. Lkb1 deficiency breaks this junctional colocalization and liberates Hepsin from desmosomes to cytosol. Moreover, the calcium switch assays demonstrate that ablation of junctional complexes is sufficient to induce cytosolic translocation of Hepsin and also that Hepsin is dispensable for the biogenesis of desmosomes. Therefore, the present data imply that loss of Lkb1 severely compromises the integrity of both apical and basolateral cellular junctions, which leads to liberation of Hepsin from desmosomal regions to cytosol. The exact mechanisms by which loss of Lkb1 compromises the integrity of cell junctions, as well as the molecular level defect liberating Hepsin, remain to be clarified by future studies. However, because Hepsin is not recruited to newly constructed desmosomes, it is possible that Hepsin is not a quintessential constituent of desmosomes but, instead, that desmosomes provide cues for spatial localization of Hepsin. In addition to AJCs and basolateral junctional complexes, the third key component controlling epithelial integrity is BM (5, 46, 47). BM represents a physical barrier for cells invading the surrounding tissue; therefore, altered BM functions influence branching of epithelial organs and invasive processes in cancer (reviewed in 37 and 36). For example, deregulation of the BM remodelling enzyme Stromelysin-1/MMP-3 simultaneously induces hyperbranching and deterioration of BM and promotes tumorigenesis in the mammary epithelium (26, 48). Our data show that Lkb1 deficiency leads to deterioration of BM and induction of hyperbranching in mammary glands and 3D mammary organoids, and that Hepsin overexpression damages both BM and epithelial architecture. Moreover, silencing of Hepsin restores BM integrity and symmetrical acinar morphology in Lkb1-deficient 3D organoids. These data strongly imply a role for Hepsin in BM remodelling and degradation. Previous studies have shown that Hepsin overexpression induces deterioration of BM in a mouse prostate cancer model (49). Furthermore, proteolytic targets of Hepsin involve BM structural and remodeling proteins, such as Laminin-332, prohepatocyte growth factor, and prourokinase plasminogen activator (38). In summary, our findings argue that loss of Lkb1 liberates Hepsin from desmosomal junctions and that the mislocalized Hepsin induces pathological deterioration of BM, which is a major contributing factor to the epithelial integrity defects observed in Lkb1-deficient epithelium.

Tumor Suppressor Function of Lkb1 Is Coupled to Epithelial Integrity Regulation. Lkb1 centrally controls metabolic, cell growth, and polarity pathways, and although altered metabolic and growth control has been implicated in Lkb1-dependent tumorigenesis (14), the role of dysregulated polarity has been anecdotal until now. The observed links between Lkb1 deficiency, BM deterioration, and mislocalization of Hepsin in mammary organoids, Myc/Lkb1- tumors, and nontumorous glands and human breast cancer samples, as well as rescue of epithelial integrity and BM by Hepsin perturbation, together infer that the epithelial integrity regulating function of Lkb1 and its tumor suppressor function are intimately coupled.

Even prolonged Myc overexpression over the time of two pregnancies in a mouse model increases the amount of epithelial cells in most glands only by promoting development of hyperplastic, multiple alveolar clusters. Each individual alveolus has an intact BM. Thus, Myc-initiated malignancies remain limited in most glands to the hyperplastic layers of epithelial cells in the alveoli because they remain separated from each other by cognate BMs. The major phenotype observed in Lkb1-deficient epithelial structures is deterioration of BM. Because misplaced and overexpressed Hepsin mediates BM breakdown in Myc/Lkb1- mammary organoids, we conclude that misregulated Hepsin is a major, but probably not the only, culprit for BM degradation in the tumor models used in this study. Therefore, we propose a model in which c-Myc mechanistically contributes to tumorigenesis by producing an excess of epithelial cells. Loss of Lkb1, for its part, deregulates Hepsin, which releases these cells from the structural boundaries established by BM (Fig. 7F). Hence, loss of a polarity gene function may become a critical cancer-promoting event, especially in the context of tumor-prone tissue composed of cells with a deregulated cell cycle.

It is conceivable that the combination of elevated expression and mislocalization of Hepsin exerts more prominent BM damaging effects than mislocalization alone; indeed, the double-Myc/Lkb1-lesion induces more prominent BM degradation than Lkb1 loss, which mislocalizes but does not evoke overexpression of Hepsin. Because Myc does not alter the position or level of Hepsin, our model predicts that Hepsin-deregulating lesions generally promote Myc-driven tumorigenesis. Indeed, prostate-targeted Hepsin has been shown to cooperate with Myc in a transgenic mouse model of prostate adenocarcinoma (50). However, such cooperation remains to be demonstrated in mouse breast cancer models, preferably using inducible systems. Finally, Hepsin overexpression is a common genetic alteration in prostate and breast cancer (41, 51), and thus a target for intensifying drug development efforts (52). The present study outlines an appropriate genetic and cellular context for biological validation of Hepsin as a potential therapeutic target in breast cancer.

Materials and Methods

Animals. All animal studies were approved by the National Animal Ethics Committee of Finland, and mice were maintained according to the protocols of the Experimental Animal Committee of the University of Helsinki. W-Myc and W-Cre mice were obtained from the Jackson Laboratory, and *Lkb1^lox* mice were kindly provided by Ron DePinho's laboratory (University of Texas MD Anderson Cancer Center, Houston, TX).

Cell Culture and Immunofluorescence. MMECs were isolated from 8- to 14-wk-old virgin female mice essentially as described previously (29). 3D organotypic culture and immunofluorescence (IF) were performed essentially as described earlier (23), with minor modifications. Detailed protocols for MMEC isolation, cell culture, IF, and quantification of 3D structures are described in *SI Materials and Methods*. Images were acquired using a Zeiss LSM Meta 510 confocal microscope.

Viral Infections. Isolated MMECs were infected on low-adhesion plates with AdCre virus using a multiplicity of infection (MOI) of 25 or with concentrated lentivirus using an MOI of 5 in DMEM/F12 growth media for 18 h as described in *SI Materials and Methods*.

Fat Pad Transplantations. Fat pad transplantations were performed essentially as described earlier (29) and in *SI Materials and Methods* by injecting 10^5 cells per gland of MMECs infected with either shControl or shLkb1-carrying lentivirus. Mice were killed 15 wk after transplantation.

www.manaraa.com

EM. 3D acini were fixed for TEM and SEM with 2% (wt/vol) glutaraldehyde in 100 mM Na-Cacodylate buffer (pH 7.4) for 1–2 h and processed subsequently for Epon embedding as described in *SI Materials and Methods*. SEM samples were visualized using a Zeiss DSM-962 microscope, and TEM samples were visualized using a Jeol 1200-EXII microscope.

Histological Staining and Histopathology. Paraffin-embedded, 5-μm-thick sections were immunostained or TUNEL-stained as described in *SI Materials and Methods*. Imaging was performed with a Leica DMB microscope and an Olympus DP50 color camera. Histopathological analysis was carried out by a pathologist (P.K.) according to the Annapolis recommendations (34). Carmine alum whole-mount staining and quantification of immunohistochemistry were performed as described in *SI Materials and Methods*.

PCR Analysis of Cre-Mediated Deletion. DNA was extracted from mammary glands using an AllPrep DNA/RNA kit (Qiagen) according to the manufacturer's instructions. PCR analysis of Cre-mediated deletion of the Lkb1^{lox} allele was performed with primers as described previously (24) and in *SI Materials and Methods*.

qPCR. RNA was isolated from MMECs using an RNeasy isolation kit (Qiagen) and from tissues using the AllPrep DNA/RNA kit according to the manufacturer's instructions and as described in *SI Materials and Methods*. Detailed information on cDNA synthesis, qPCR reaction, and primers can be found in *SI Materials and Methods*.

Patient Material. Human breast tumor samples were obtained from diagnostic material sent to the pathology laboratory of the University of Helsinki Central Hospital in conjunction with elective surgery. The study was approved by the Helsinki University Hospital Ethics Committee.

1. Lee M, Vasioukhin V (2008) Cell polarity and cancer—Cell and tissue polarity as a non-canonical tumor suppressor. *J Cell Sci* 121:1141–1150.
2. Bryant DM, Mostov KE (2008) From cells to organs: Building polarized tissue. *Nat Rev Mol Cell Biol* 9:887–901.
3. Shin K, Fogg VC, Margolis B (2006) Tight junctions and cell polarity. *Annu Rev Cell Dev Biol* 22:207–235.
4. Delva E, Tucker DK, Kowalczyk AP (2009) The desmosome. *Cold Spring Harb Perspect Biol* 1:a002543.
5. Yurchenco PD, Amenta PS, Patton BL (2004) Basement membrane assembly, stability and activities observed through a developmental lens. *Matrix Biol* 22:521–538.
6. Huang L, Muthuswamy SK (2010) Polarity protein alterations in carcinoma: A focus on emerging roles for polarity regulators. *Curr Opin Genet Dev* 20:41–50.
7. Partanen JI, Nieminen AI, Klefstrom J (2009) 3D view to tumor suppression: Lkb1, polarity and the arrest of oncogenic c-Myc. *Cell Cycle* 8:716–724.
8. Bilder D, Li M, Perrimon N (2000) Cooperative regulation of cell polarity and growth by Drosophila tumor suppressors. *Science* 289:113–116.
9. Pagliarini RA, Xu T (2003) A genetic screen in Drosophila for metastatic behavior. *Science* 302:1227–1231.
10. Brumby AM, Richardson HE (2003) scribble mutants cooperate with oncogenic Ras or Notch to cause neoplastic overgrowth in Drosophila. *EMBO J* 22:5769–5779.
11. Bilder D (2004) Epithelial polarity and proliferation control: Links from the Drosophila neoplastic tumor suppressors. *Genes Dev* 18:1909–1925.
12. Dolberg DS, Bissell MJ (1984) Inability of Rous sarcoma virus to cause sarcomas in the avian embryo. *Nature* 309:552–556.
13. Goldstein B, Macara IG (2007) The PAR proteins: Fundamental players in animal cell polarization. *Dev Cell* 13:609–622.
14. Shackelford DB, Shaw RJ (2009) The LKB1-AMPK pathway: Metabolism and growth control in tumour suppression. *Nat Rev Cancer* 9:563–575.
15. Martin SG, St Johnston D (2003) A role for Drosophila LKB1 in anterior-posterior axis formation and epithelial polarity. *Nature* 421:379–384.
16. Mirouse V, Swick LL, Kazgan N, St Johnston D, Brenman JE (2007) LKB1 and AMPK maintain epithelial cell polarity under energetic stress. *J Cell Biol* 177:387–392.
17. Baas AF, et al. (2004) Complete polarization of single intestinal epithelial cells upon activation of LKB1 by STRAD. *Cell* 116:457–466.
18. Hezel AF, et al. (2008) Pancreatic LKB1 deletion leads to acinar polarity defects and cystic neoplasias. *Mol Cell Biol* 28:2414–2425.
19. Katajisto P, et al. (2007) The LKB1 tumor suppressor kinase in human disease. *Biochim Biophys Acta* 1775:63–75.
20. Wingo SN, et al. (2009) Somatic LKB1 mutations promote cervical cancer progression. *PLoS ONE* 4:e5137.
21. Hezel AF, Bardeesy N (2008) LKB1; linking cell structure and tumor suppression. *Oncogene* 27:6908–6919.
22. Meyer N, Penn LZ (2008) Reflecting on 25 years with MYC. *Nat Rev Cancer* 8:976–990.
23. Partanen JI, Nieminen AI, Mäkelä TP, Klefstrom J (2007) Suppression of oncogenic properties of c-Myc by LKB1-controlled epithelial organization. *Proc Natl Acad Sci USA* 104:14694–14699.
24. Bardeesy N, et al. (2002) Loss of the Lkb1 tumour suppressor provokes intestinal polyposis but resistance to transformation. *Nature* 419:162–167.
25. Ewald AJ, Brenot A, Duong M, Chan BS, Werb Z (2008) Collective epithelial migration and cell rearrangements drive mammary branching morphogenesis. *Dev Cell* 14:570–581.
26. Sympson CJ, et al. (1994) Targeted expression of stromelysin-1 in mammary gland provides evidence for a role of proteinases in branching morphogenesis and the requirement for an intact basement membrane for tissue-specific gene expression. *J Cell Biol* 125:681–693.
27. Wagner KU, et al. (1997) Cre-mediated gene deletion in the mammary gland. *Nucleic Acids Res* 25:4323–4330.
28. Robinson GW, McKnight RA, Smith GH, Hennighausen L (1995) Mammary epithelial cells undergo secretory differentiation in cycling virgins but require pregnancy for the establishment of terminal differentiation. *Development* 121:2079–2090.
29. Welm BE, Dijkgraaf GJ, Bledau AS, Welm AL, Werb Z (2008) Lentiviral transduction of mammary stem cells for analysis of gene function during development and cancer. *Cell Stem Cell* 2:90–102.
30. McCarthy A, et al. (2009) Conditional deletion of the Lkb1 gene in the mouse mammary gland induces tumour formation. *J Pathol* 219:306–316.
31. Sandgren EP, et al. (1995) Inhibition of mammary gland involution is associated with transforming growth factor alpha but not c-myc-induced tumorigenesis in transgenic mice. *Cancer Res* 55:3915–3927.
32. Schoenenberger CA, et al. (1988) Targeted c-myc gene expression in mammary glands of transgenic mice induces mammary tumours with constitutive milk protein gene transcription. *EMBO J* 7:169–175.
33. Rose-Hellekant TA, Sandgren EP (2000) Transforming growth factor alpha- and c-myc-induced mammary carcinogenesis in transgenic mice. *Oncogene* 19:1092–1096.
34. Cardiff RD, et al. (2000) The mammary pathology of genetically engineered mice: The consensus report and recommendations from the Annapolis meeting. *Oncogene* 19: 968–988.
35. D'Cruz CM, et al. (2001) c-MYC induces mammary tumorigenesis by means of a preferred pathway involving spontaneous Kras2 mutations. *Nat Med* 7:235–239.
36. Fata JE, Werb Z, Bissell MJ (2004) Regulation of mammary gland branching morphogenesis by the extracellular matrix and its remodeling enzymes. *Breast Cancer Res* 6:1–11.
37. Lu P, Sternlicht MD, Werb Z (2006) Comparative mechanisms of branching morphogenesis in diverse systems. *J Mammary Gland Biol Neoplasia* 11:213–228.
38. Bugge TH, Antalis TM, Wu Q (2009) Type II transmembrane serine proteases. *J Biol Chem* 284:23177–23181.
39. Mackman RL, et al. (2001) Exploiting subsite S1 of trypsin-like serine proteases for selectivity: Potent and selective inhibitors of urokinase-type plasminogen activator. *J Med Chem* 44:3856–3871.
40. Miao J, et al. (2008) Hepsin colocalizes with desmosomes and induces progression of ovarian cancer in a mouse model. *Int J Cancer* 123:2041–2047.
41. Dhanasekaran SM, et al. (2001) Delineation of prognostic biomarkers in prostate cancer. *Nature* 412:822–826.
42. Fenton H, et al. (2006) LKB1 protein expression in human breast cancer. *Appl Immunohistochem Mol Morphol* 14:146–153.
43. Bignell GR, et al. (1998) Low frequency of somatic mutations in the LKB1/Peutz-Jeghers syndrome gene in sporadic breast cancer. *Cancer Res* 58:1384–1386.
44. Shen Z, Wen XF, Lan F, Shen ZZ, Shao ZM (2002) The tumor suppressor gene LKB1 is associated with prognosis in human breast carcinoma. *Clin Cancer Res* 8:2085–2090.
45. Amin N, et al. (2009) LKB1 regulates polarity remodeling and adherens junction formation in the Drosophila eye. *Proc Natl Acad Sci USA* 106:8941–8946.
46. Slade MJ, Coope RC, Gomm JJ, Coombes RC (1999) The human mammary gland basement membrane is integral to the polarity of luminal epithelial cells. *Exp Cell Res* 247:267–278.
47. Petersen OW, Rønnov-Jessen L, Howlett AR, Bissell MJ (1992) Interaction with basement membrane serves to rapidly distinguish growth and differentiation pattern of normal and malignant human breast epithelial cells. *Proc Natl Acad Sci USA* 89: 9064–9068.
48. Sternlicht MD, et al. (1999) The stromal proteinase MMP3/stromelysin-1 promotes mammary carcinogenesis. *Cell* 98:137–146.
49. Klezovitch O, et al. (2004) Hepsin promotes prostate cancer progression and metastasis. *Cancer Cell* 6:185–195.
50. Nandana S, et al. (2010) Hepsin cooperates with MYC in the progression of adenocarcinoma in a prostate cancer mouse model. *Prostate* 70:591–600.
51. Xing P, et al. (2011) Clinical and biological significance of hepsin overexpression in breast cancer. *J Investig Med* 59:803–810.
52. Chevillet JR, Park GJ, Bedalov A, Simon JA, Vasioukhin VI (2008) Identification and characterization of small-molecule inhibitors of hepsin. *Mol Cancer Ther* 7:3343–3351.

Partanen et al.